Journal of Applied Electrochemistry **30**: 973–979, 2000.

Inhibition of CuNi10Fe corrosion in seawater by sodium-diethyl-dithiocarbamate: an electrochemical and analytical study

LJ. ALJINOVIĆ, S. GUDIĆ and M. ŠMITH
Faculty of Chemical Technology, Department of Electrochemistry and Materials Protection, Teslina 10/V, 21000 Split, Croatia

Received 22 September 1999; accepted in revised form 25 January 2000

Key words: CuNi10Fe, inhibition, natural seawater, sodium-diethyl-dithiocarbamate

Abstract

The efficiency of sodium-diethyl-dithiocarbamate (NaDDTC) as corrosion inhibitor for CuNi10Fe alloy was studied in natural seawater by means of immersion tests, polarization measurements, electrochemical impedance spectroscopy (EIS) and Auger electron spectroscopy (AES). After immersion of the alloy for 24 h in various concentrations of NaDDTC, layers were formed which act as a physical barrier to the corrosion attack. The polarization curves obtained with electrodes in seawater indicate retardation of both the anodic and cathodic processes. From EIS measurements equivalent circuits, which illustrate the behaviour of the reaction product film, were proposed and individual circuit elements at the open circuit potential and anodic polarization were defined. The results obtained for inhibitor efficiency from weight losses, corrosion currents and from impedance measurements are in fair agreement. The inhibition film does not lose efficiency even at anodic polarization, although the AES measurements indicate a change in the organic molecule structure. The hypothesis proposed is that a possible reconstruction of the organic molecule takes place, with release of CS_2.

1. Introduction

Copper–nickel alloys show good resistance to corrosion and fouling [1], have good heat transfer properties and machinability and find much use in marine applications owing to these properties and their relatively low cost [2]. Their good corrosion resistance may be attributed to a protective layer consisting mainly of a thin, strongly adherent inner Cu_2O film which is in contact with the electrolyte through a porous and thick outer layer [3]. Its composition and thickness depend on anions present in the electrolyte and on the growth time. Formation of paratacamite with Cl^- ions and brochantite with SO_4^{2-} ions is possible in seawater, and after longer exposure, other salts or oxide types are found [4]. Several studies have pointed out the problem of corrosion of these alloys caused by seawater flow, local turbulence and galvanic coupling [5], pollution with sulfides [6–8] and active chlorine [9], and also temperature variations [10, 11].

To improve the protective properties of the naturally formed surface layer, specific organic molecules may be added as corrosion inhibitors [12]. The inhibition mechanism depends on the ability of the organic molecule to be adsorbed or to form sparingly soluble complexes with metal cations and their polymerization properties. This is essential in almost neutral aerated chloride solutions, where no true passivation layer can be expected on the metal surface, because chloride 'contaminated oxide' [13] permits the passage of metal cations through it.

In previous work [14, 15], the d.c., AES and XPS examinations were applied to investigate the efficiency of NaDDTC as inhibitor for CuNi10Fe alloy in chloride solutions. It was established that inhibition properties depended on inhibitor concentration, aeration and hydrodynamic conditions of the electrolyte.

As more quantitative information on inhibition may be obtained by a.c. impedance measurements, in the present study this technique has been applied to obtain a better insight into the behaviour of NaDDTC as inhibitor for CuNi10Fe alloy in natural seawater.

2. Experimental details

All measurements were made on the alloy with the composition (%): Cu 87.62, Ni 10.89 and Fe 2.40. Electrodes were cut from a pipe of 50 mm outer diameter to the size of 20×20 mm. The outer surface, edges and contacts with Cu-wire were carefully covered with epoxy resin. The inner concave surface was prepared for inhibitor deposition or electrochemical examinations by successive mechanical polishing with SiC abrasive paper up to 600 grade until a planar surface was obtained. This was followed by degreasing

in acetone for 1 min, pickling in 25 vol% HNO_3 for 5 s and rinsing with doubly distilled water and drying in a steam of N_2 [16]. The exposed area was 3.24 cm^2. Immediately after this procedure the electrodes were immersed into the stirred solution open to atmosphere for 24 h at $25 \pm 1\,^{\circ}C$. The concentrations of inhibitor were 8.88×10^{-4}, 17.8×10^{-4} and 26.6×10^{-4} M. After deposition of the inhibitor layer on the surface, electrodes were left in air in laboratory conditions to dry and for a more stable film to be achieved. This procedure formed a reddish–brown film with good adhesion to the surface. The efficiency of NaDDTC as corrosion inhibitor for CuNi10Fe alloy was examined in natural seawater from an uninhabited part of the Adriatic coast (pH 8.15). A conventional three-compartment Pyrex cell was used with a large platinum sheet and a saturated calomel electrode (SCE) serving as the counter and the reference electrodes, respectively.

The concentration of Cu, Ni, and Fe dissolved from both unprotected and protected samples was determined in 1 L of electrolyte after 5 h polarization at +100 mV and after 45 h immersion at open circuit potential (o.c.p.) by means of atomic absorption spectroscopy (Perkin Elmer 703). Three independent probes with a blank probe were analysed for each of the samples examined.

Polarization and impedance measurements were carried out in stationary conditions where the electrolyte was open to the laboratory air. The impedance spectra were performed on the fixed electrode at the o.c.p. and at polarization of +50 and +100 mV from the o.c.p. The frequency range studied was 30 mHz to 50 kHz with the perturbation signal amplitude $\Delta E = 10$ mV. These measurements were performed using a potentiostat PAR M273, and a lock-in amplifier PAR M5210 controlled by a personal computer.

An Auger-ESCA device (PHY SAM 545A) was used to analyse the presence of elements characteristic for the inhibitor molecules.

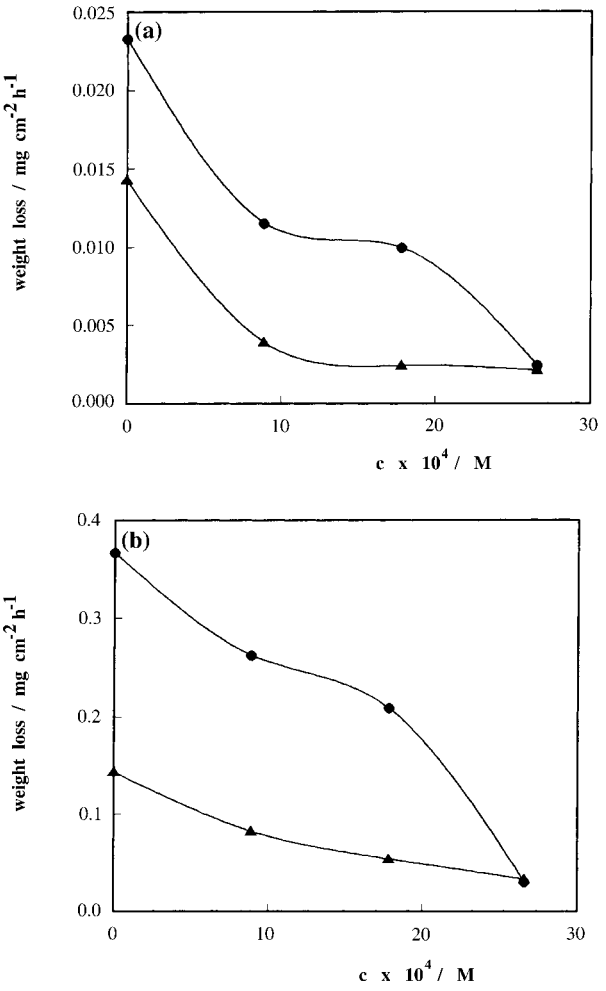

Fig. 1. Corrosion rate of Cu (●) and Ni (▲) from the electrode surface treated with various inhibitor concentrations: (a) 45 h immersion at o.c.p. and (b) 5 h anodic polarization at +100 mV.

3. Results

3.1. *Weight loss measurements*

Figure 1(a) and (b) shows the corrosion rate data obtained from concentrations of dissolved Cu and Ni, while Table 1 shows their ratio in 1 L of the electrolyte for both unprotected and protected electrodes at o.c.p. and at +100 mV of anodic polarization. As expected, the weight loss is higher under anodic polarization. Iron was not found even in trace amounts, which is probably due to its specific function in the alloy [17].

The percentage inhibition efficiency (η_{ie}) was calculated according to:

$$\eta_{ie} = \left(\frac{x_0 - x_1}{x_0}\right) \times 100 \qquad (1)$$

where x_0 and x_1 represent weight loss for the uninhibited and the inhibited electrode, respectively. The results are summarized in Table 1 together with η_{ie} data obtained from polarization and EIS measurements.

3.2. *Polarization measurements*

Polarization curves were recorded to obtain information about the influence of NaDDTC on anodic and cathodic processes. Protected and unprotected electrodes were polarized after immersion in the electrolyte for 1 h in contact with the laboratory air to establish the corrosion potential. The measurements started from −250 mV via o.c.p. to +250 mV. The scan rate was 0.5 mV s^{-1}. The results are presented in Figure 2. With increasing NaDDTC concentrations, the cathodic and anodic polarization curves are shifted towards lower currents, indicating that NaDDTC reduces anodic dissolution of the alloy and also hinders cathodic reduction of oxygen.

The inhibition efficiency (η_{ie}) was calculated according to Equation 1. In this case x_0 and x_1 represent corrosion current densities for the uninhibited and inhibited

Table 1. Values of Cu/Ni ratio and inhibition efficiencies η_{ie} of NaDDTC in the seawater for the various treated CuNi10Fe alloy Theoretical Cu/Ni ratio for the alloy is 8.51.

$c \times 10^4$/M	o.c.p.				+100 mV from o.c.p.			
	Cu/Ni	η_{ie}/%			Cu/Ni	η_{ie}/%		
		Weight loss	Polarization measurements	Impedance measurements		Weight loss	Polarization measurements	Impedance measurements
0	1.63	–	–	–	2.52	–	–	–
8.88	2.96	59.04	10.00	66.8	3.20	32.38	69.64	–
17.80	4.11	67.29	88.37	79.6	3.90	48.51	89.31	–
26.60	1.15	88.03	89.14	83.3	0.92	87.94	96.94	98.90

electrode, respectively. The results are presented in Table 1.

3.3. *Impedance measurements*

3.3.1. *Influence of inhibitor concentration*

The results of impedance measurements on inhibitor free CuNi10Fe electrodes and electrodes previously treated with various concentrations of inhibitor at the o.c.p. are shown in Figure 3 in the form of Nyquist and Bode plots. The response of the system in the Nyquist complex plane (Figure 3(a)) is a semi-circle whose diameter increases with the increase in inhibitor concentration. A more convenient method, which shows the frequency dependence of the impedance data better, is the Bode diagram (Figure 3(b)). In the presence of inhibitor, the shapes of the impedance curves are very similar. The high frequency limit ($f > 1$ kHz) corresponds to the electrolyte resistance, R_{el}. The low frequency limit ($f < 1$ Hz) represents the sum of R_{el} and the resistance R_1, which determines polarization resistance for dissolution processes. In these two borderline cases the phase angle between the current and the potential, θ, assumes a value of about 0°, corresponding to the resistive behaviour of R_{el} and $(R_{el} + R_1)$.

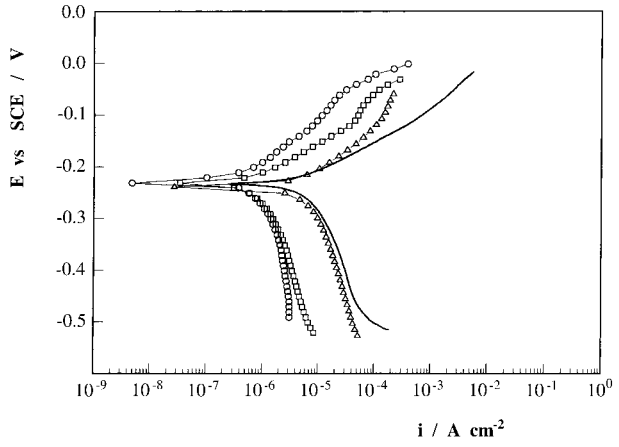

Fig. 2. Polarization curves for unprotected and protected CuNi10Fe electrodes with different concentration of NaDDTC in seawater. Key: (——) unprotected; (△) 8.88×10^{-4}, (□) 17.80×10^{-4} and (○) 26.60×10^{-4} M.

At medium frequencies the capacitive behaviour of the system is evident and is determined by the dielectric properties of the surface layer consisting of sparingly soluble corrosion products alone or incorporated with the CuDDTC complex. A slope of the Bode straight line of about −1 is characteristic for this frequency range. The phase shift between current and voltage approaches a value of about −80°.

It is clearly seen that the centre of the semicircle does not lie on the real axis. The depression of the capacitive semicircle observed may be treated as surface non-homogeneity of the polycrystalline solid electrode due to surface roughness [18], to insufficient polishing and to

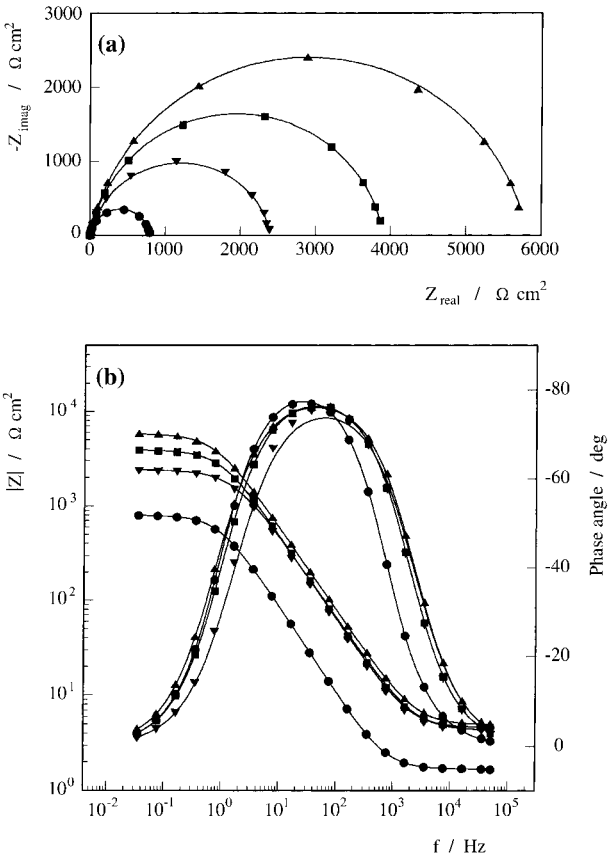

Fig. 3. Nyquist (a) and Bode (b) plots for unprotected (●) and protected CuNi10Fe electrode with (▼) 8.88×10^{-4}, (■) 17.8×10^{-4} and (▲) 26.6×10^{-4} M NaDDTC at o.c.p.

corrosion, grain boundaries [19], to impurities and to the fractal nature of the surface [20]. This allows for introduction of the constant phase element (CPE) instead of an 'ideal' capacitor to account for the deviations observed. The impedance of the constant phase element, Z_{CPE}, is described in [21, 22]:

$$Z_{CPE} = [Q(j\omega)^n]^{-1} \quad (2)$$

where Q is constant. The parameter n is also a constant that can assume different values in the range from -1 to $+1$. According to the magnitude of the value n, Equation 2 can describe inductance ($n = -1$), resistance ($n = 0$), Warburg impedance ($n = 0.5$) and capacitance ($n = 1$).

For all the examined electrode/electrolyte and electrode/inhibitor/electrolyte systems, the value of the parameter n determined (Table 2) indicates that the CPE replaces capacitance in the equivalent circuit proposed in Figure 4(a).

The experimental data, R_{el}, Q and R_1, were found to be sufficiently well fitted by the transfer function of the proposed equivalent circuit within the experimental error. The data presented in Table 2 show that an increase in inhibitor concentration causes a decrease in capacitance and a increase in resistance of one order of magnitude, which indicates the protective properties of the surface layer. When the inhibitor concentration increases up to 26.6×10^{-4} M the resistance increases from 796.70 to 5808.40 Ω cm^2. The capacitance value obtained without inhibitor is much higher than those observed in the presence of the NaDDTC layer. The high value of capacitance for the inhibitor free electrode (256.82×10^{-6} Ω^{-1} s^n cm^{-2}) may be attributed to the presence of the corrosion product film, mainly Cu_2O, which induces a considerable increase in the specific surface area [23]. The capacitance for the protected electrode with different concentrations of NaDDTC under the same conditions were found to be in the range (55.71–43.61) $\times 10^{-6}$ Ω^{-1} s^n cm^{-2}.

The total resistance of the system was used to calculate η_{ie} for NaDDTC in seawater according to Equation 1. In this case x_0 and x_1 represent the total resistance with and without inhibitor, respectively. The results obtained are presented in Table 1.

3.3.2. *Influence of anodic polarization*

Figure 5 presents the impedance spectra of unprotected CuNi10Fe electrodes in seawater at different anodic potentials (+50 and +100 mV from the o.c.p.) with the measurements made at open circuit potential. As mentioned earlier, the Nyquist plot shows a semicircular capacitive loop at the o.c.p. in the whole frequency range. An increase in anodic polarization causes a marked decrease in overall impedance. With the increase

Table 2. Impedance parameters for unprotected and protected CuNi10Fe alloy in seawater at open circuit potential

$c \times 10^4$ /M	R_{el} /Ω cm^2	$Q \times 10^6$ /Ω^{-1} s^n cm^{-2}	n	R_1 /Ω cm^2
0	1.68	256.82	0.92	796.70
8.88	4.29	55.71	0.89	2400.30
17.80	4.58	51.20	0.89	3900.30
26.60	4.89	43.61	0.88	5808.40

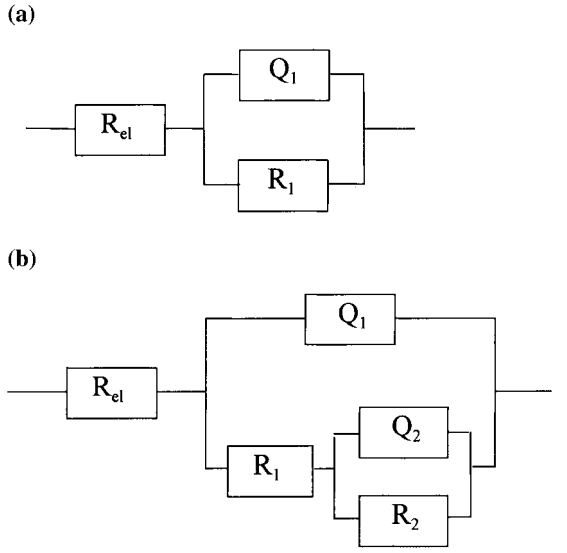

Fig. 4. Equivalent circuits for modelling impedance data of the CuNi10Fe alloy.

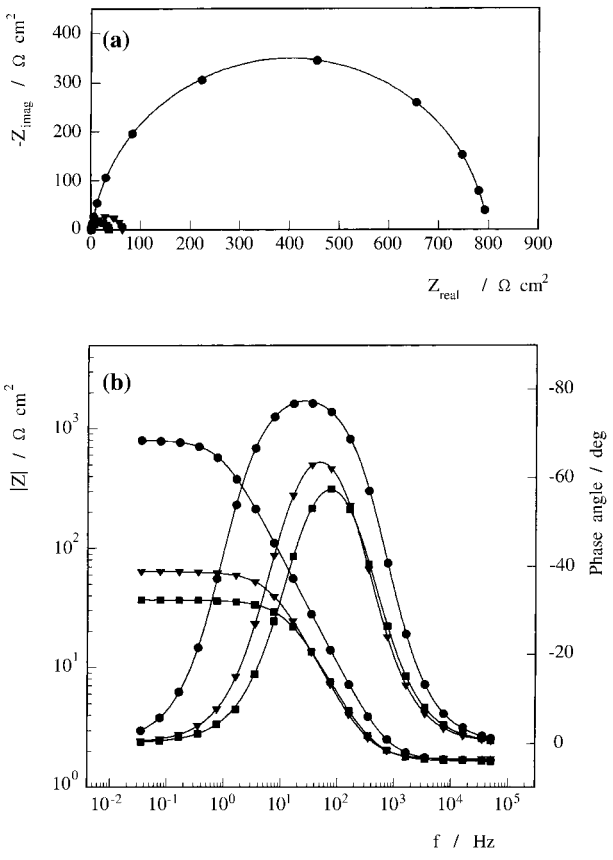

Fig. 5. Nyquist (a) and Bode (b) plots for unprotected CuNi10Fe electrodes at (●) o.c.p., (▼) +50 mV and (■) +100 mV anodic polarization.

Table 3. Impedance parameters for unprotected and protected (with 26.6×10^{-4} M NaDDTC) CuNi10Fe alloy in seawater at different anodic polarization

	R_{el} /Ω cm^2	$Q_1 \times 10^6$ /Ω^{-1} s^n cm^{-2}	n_1	R_1 /Ω cm^2	$Q_2 \times 10^6$ /Ω^{-1} s^n cm^{-2}	n_2	R_2 /Ω cm^2
unprotected electrode							
+50 mV	1.72	564.43	0.91	62.12	–	–	–
+100 mV	1.65	571.97	0.89	35.22	–	–	–
protected electrode							
+50 mV	4.44	56.48	0.85	1811.15	437.48	0.74	2784.00
+100 mV	5.01	64.73	0.86	1297.18	467.36	0.81	1750.25

in the polarization potential to +50 and +100 mV from the o.c.p., metal dissolution is accelerated, resulting in accumulation of corrosion products and consequent adsorption on the metal surface. In this case, the capacitive loop is dominant with the parallel arrangement of reaction resistance and double layer capacitance. The experimental data were fitted to the equivalent circuit in Figure 4(a), and Table 3 shows the characteristic values. With increase in anodic polarization, resistance decreased by more than one order of magnitude, while capacity values were found to be two times higher than the value recorded at the o.c.p. The high value of capacitance (i.e., $Q = 571.97 \times 10^{-6}$ Ω^{-1} s^n cm^{-2}) may be attributed to the presence of the corrosion product film.

However, for electrodes with an inhibitor film, the corrosion starts preferentially in defects and pores in the protective layer.

The impedance spectra obtained at different potentials on the alloy protected with 26.6×10^{-4} M NaDDTC (at o.c.p., +50 and +100 mV anodic polarization) are presented in Figure 6. Obviously, the inhibitor layer exhibits a purely capacitive impedance behaviour at the o.c.p., the modulus of the impedance at a low frequency being about $|Z| \simeq 6$ kΩ cm^2. When anodic polarization increases, an additional time constant appears in the medium frequency range revealing the development of 'active pores'. At anodic polarization, the absolute value (modulus) of the impedance decreases substantially, indicating reduced corrosion protection.

The experimental fitting obtains fairly good results for use of the equivalent circuit shown in Figure 4(b), which proposes introduction of two time constants. The first time constant is attributed to the protective layer of the inhibitor on the surface and is described by the layer capacitance C_1 and the layer resistance R_1, which is representative of the electrolyte reaching the metal substrate through a defect in the layer. The second loop is determined by the charge transfer resistance R_2 and by the double layer capacitance C_2 due to defects in the inhibitor layer. All the capacitance shown in the equivalent circuit has been modeled mathematically using a constant phase element. Table 3 presents the results obtained.

In comparison with the unprotected electrode where anodic dissolution already takes place at the polarization of +50 mV, the protective action was observed here until higher anodic polarization values. Taking into account the results obtained, under anodic polarization a change in the structure of the protective film probably takes place, and unprotected spots form on the electrode.

3.4. *Surface analysis*

The depth profiles in Figure 7 show how the percentage atomic concentration of oxygen, copper, and elements from the organic molecules (N, S, C) vary with the depth of penetration of the etching ion beam through the surface film before and after anodic polarization. It can be seen that, after anodic polarization, the share of sulfur and carbon decreases while the share of nitrogen remains unchanged. Chlorine, present throughout the profile is omitted for greater clearness.

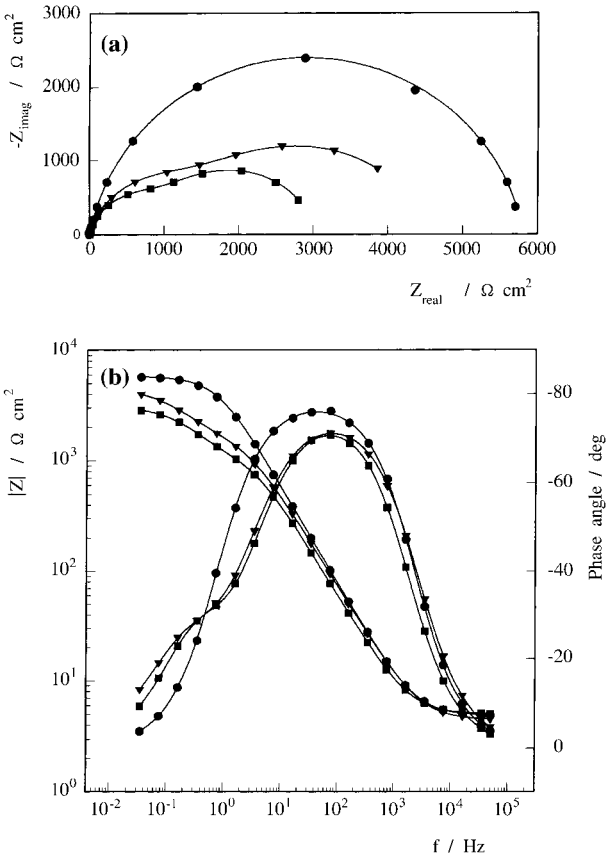

Fig. 6. Nyquist (a) and Bode (b) plots for CuNi10Fe electrode protected with 26.6×10^{-4} M NaDDTC inhibitor at (●) o.c.p., (▼) +50 mV and (■) +100 mV anodic polarization.

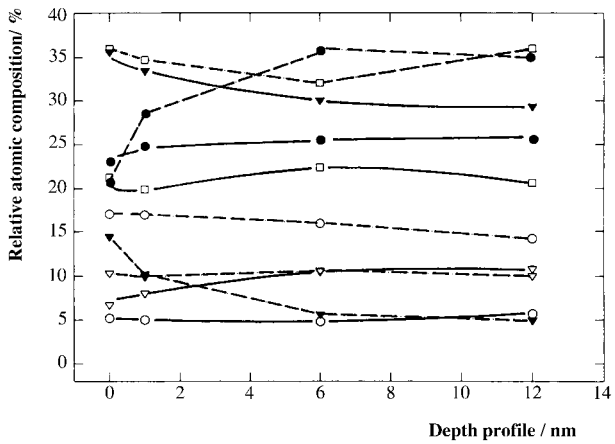

Fig. 7. AES depth profiles for protected CuNi10Fe coupons with 26.6×10^{-4} M NaDDTC before (- - - - -) and after 5 h polarization at +100 mV (——). Key: (○) S, (●) C, (▽) N, (▼) O and (□) Cu.

As nickel peaks in the AAS spectra appear at approximately the same locations as some of the copper peaks, nickel has not been recorded in the surface layer by this method.

4. Discussion

This study has examined the efficiency of NaDDTC as corrosion inhibitor for the CuNi10Fe alloy in seawater at the o.c.p. and at the anodic polarization of +50 and +100 mV. The results obtained have confirmed NaDDTC to be an efficient inhibitor and to retard anodic dissolution of the metal and hinder cathodic oxygen reduction.

Results in Table 1 compare the theoretical Cu/Ni ratios for the alloy with those obtained by weight loss measurements. In the case of the electrode inhibited with 26.6×10^{-4} M NaDDTC, the ratio obtained is lower than the theoretical value and than that for uninhibited electrodes. This points to a conclusion that the $DDTC^-$ anions prevent dissolution of copper with which they form a complex compound. The film formed acts as a physical barrier to alloy dissolution. This Table also summarizes the data on inhibition efficiency obtained from the immersion tests, corrosion currents at o.c.p. and +100 mV polarization as well as from EIS data. The best protection is obtained at the inhibitor concentration of 26.6×10^{-4} M.

It is generally accepted that the corrosion resistance of copper–nickel alloys at the o.c.p. can be attributed to formation of an adherent copper(I)oxide [3] and a nickel oxide phase underlying the cuprous oxide. For longer exposure times, cupric compounds cover the surface. In our case, during immersion of the electrode in the solution of NaDDTC in order for the protective film to be formed, a Cu_2O film was formed at the same time as the Cu-complex settled. The electrode surface coverage by the Cu-complex depends on the concentration of the NaDDTC in the solution.

As most cuprous compounds adopt tetrahedral coordination in both discrete ions or molecules and in polymeric structures found in the crystalline state, a multilayer structure may be formed with $DDTC^-$ anions. According to [24] the diethyldithiocarbamate molecules are bound to four faces of the Cu tetrahedron via sulfur atoms; one sulfur atom is bound to two copper atoms and the second sulfur atom to the third copper atom of a tetrahedron face. The proposed bonding is shown in Figure 8(a) schematically.

The presence of all the elements of the organic molecule (with copper and oxygen) at the protected alloy confirms the surface film structure proposed. Dissolution of Cu and Ni during free corrosion for a longer period of time (45 h) includes mass transport of Cu and Ni ions through the oxide parts of the protective layer.

Although the weight loss under anodic polarization is much higher than that at free corrosion, the inhibition efficiency is still very high. Results shown in Figure 7 indicate that after anodic polarization there occurred a change in the ratio of the elements forming the organic molecule. The share of C and S is smaller, while that of N is equal to that before anodic polarization. The AES analysis in the complex protected alloy/seawater system cannot determine actual quantitative ratios for individual elements in a molecule. However, the data shown in Figure 7, a smell of CS_2 separated at polarization, and the fact that the bonding potential of the alkylthio group is lower than that of the $-NH_2$ group [24] provided confirmation for the model proposed in Figure 8(b). Thus, after separation of CS_2, the remaining part of the molecule is bound to only one copper atom via nitrogen, leaving, on average, two Cu atoms from the tetrahedron face unbound. Owing to two ethyl groups, the electrode coverage is still high, but these weakened parts of the protective layer make possible the dissolution of the alloy components under these circumstances. The emergence of the second time constant at anodic polarization (Figure 6) confirms the mechanism proposed. The first time constant is related to the presence of the Cu-complex(es) as inhibitor while the second one includes charge transport of Cu and Ni ions.

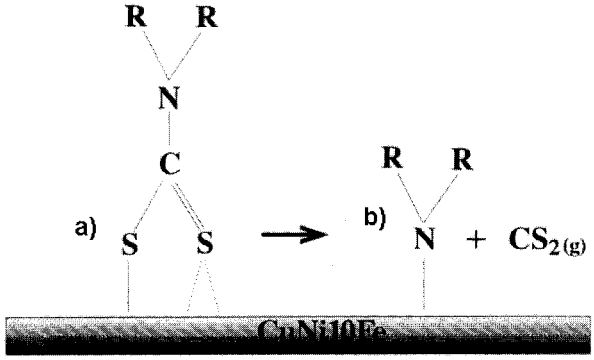

Fig. 8. Proposed protective layer structure (a) and decomposition of the diethyl-dithiocarbamate molecule after anodic polarization (b).

The experimental observations show that NaDDTC does not alter the electrochemical reactions responsible for corrosion. It inhibits corrosion primarily through formation of an interphase protective inhibitor layer that acts as a physical barrier to impede the attack of the medium. Namely, NaDDTC as inhibitor of CuNi10Fe corrosion was incorporated into defects of the surface oxide layer. The large area of the complex compound molecule closes the pores of the oxide layer forming a more compact protective layer.

5. Conclusion

The surface analysis and electrochemical measurements have shown that when CuNi10Fe alloy is exposed to a NaDDTC solution, a multilayer complex structure is formed at the surface with two sulfur atoms for each organic molecule. The impedance spectra were obtained at the o.c.p. and at anodic polarization for both unprotected and protected electrodes. The equivalent circuit parameters obtained at o.c.p. show that resistance of the surface layer increases with the NaDDTC concentration.

At anodic polarization, the second time constant was observed as a consequence of dissolution at weak parts of the surface due to rearrangement of the organic molecule.

References

1. C.A. Powell, *Oebalia* **19** (1993) 323.
2. A. Cohen, 'Copper and copper base alloy' in *Process Industries Corrosion*, (1988) 479.
3. C. Kato, J.E. Castle, B.G. Ateya and H.W. Pickering, *J. Electrochem. Soc.* **127** (1980) 1897.
4. C. Fiaud, *Proc. 8th SEIC*, Ferrara (1995), p. 929.
5. F.P. IJsseling, *Corros. Sci.* **14** (1974) 97.
6. P.K. Chanhan and H.S. Gadyar, *Corros. Sci.* **25** (1985) 55.
7. B.C. Syrett and S.S. Wing, *Corrosion NACE* **36** (1980) 73.
8. L.E. Eiselstein, B.C. Syrett, S.S. Wing and R.D. Caligiuri, *Corros. Sci.* **23** (1983) 223.
9. R. Francis, *Corros. Sci.* **26** (1986) 205.
10. R. Francis, *Br. Corros. J.* **18** (1983) 35.
11. Y.Z. Wang, A.M. Beccaria and G. Poggi, *Corros. Sci.* **36** (1994) 1277.
12. G. Trabanelli, 'Corrosion inhibitors', F. Mansfield (Ed.), *in* '*Corrosion Mechanisms*' (Marcel Dekker, New York, 1987), p. 119.
13. M. Metikoš-Huković, R. Babić and Z. Grubač, *J. Appl. Electrochem.* **28** (1998) 433.
14. Lj. Aljinović, J. Radošević, M. Šmith and M. Kliškić, *Oebalia* **19** (1993) 567.
15. Lj. Aljinović, M. Šmith, V. Gotovac and Z. Hell, *Proc. 7th SEIC*, Ferrara (1990) 1091.
16. D.E. Dobb, J.P. Storvick and G.K. Pagenkopf, *Corros. Sci.* **26** (1986) 525.
17. M. Pourbaix, *Corros. Sci.* **12** (1972) 161.
18. R. De Levie, *Electrochim. Acta* **10** (1965) 113.
19. F.B. Growcock and R.J. Jasinski, *J. Electrochem. Soc.* **136** (1989) 2310.
20. W.H. Mulder and J.A. Sluyters, *Electrochim. Acta* **33** (1988) 333.
21. I.D. Raistrick, J.R. Macdonald and D.R. Franceschetti, 'Theory' *in* J.R. Macdonald (Ed.), '*Impedance Spectroscopy*' (J. Wiley & Sons, New York, 1987).
22. Z. Stoynov, *Electrochim. Acta* **35** (1990) 1493.
23. A. Bonnel, F. Dabosi, C. Deslouis, M. Duprat, M. Keddam and B. Tribollet, *J. Electrochem. Soc.* **130** (1983) 753.
24. A.G. Massey, 'Copper' *in* A.F. Trotman-Dickenson (Ed.), '*Comprehensive Inorganic Chemistry*' (Pergamon Press, Oxford, 1973), p. 1.